Journal Pre-proof

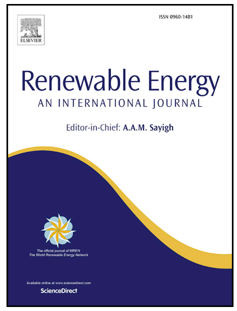

Quantifying energy symbiosis of building-integrated agriculture in a mediterranean rooftop greenhouse

Joan Muñoz-Liesa, Mohammad Royapoor, Elisa López-Capel, Eva Cuerva, Martí Rufí-Salís, Santiago Gassó-Domingo, Alejandro Josa

PII: S0960-1481(20)30630-3

DOI: https://doi.org/10.1016/j.renene.2020.04.098

Reference: RENE 13427

To appear in: *Renewable Energy*

Received Date: 14 January 2020

Revised Date: 15 April 2020

Accepted Date: 18 April 2020

Please cite this article as: Muñoz-Liesa J, Royapoor M, López-Capel E, Cuerva E, Rufí-Salís Martí, Gassó-Domingo S, Josa A, Quantifying energy symbiosis of building-integrated agriculture in a mediterranean rooftop greenhouse, *Renewable Energy* (2020), doi: https://doi.org/10.1016/j.renene.2020.04.098.

CRediT author statement

All authors were responsible for the conceptualitzation of the study, writing review & editing. **J. Muñoz-Liesa, M. Royapoor** Software, Validation, Formal analysis; **J. Muñoz-Liesa, M. Royapoor, E. López-Capel, E. Cuerva, M. Rufí-Salís** Investigation, Resources; **J. Muñoz-Liesa** Writing original draft, Data curation, Visualtization; **E. Cuerva, S. Gassó-Domingo, A.Josa** Supervision, Project administration, funding acquisition. All authors critically revised the draft for important intellectual content. All authors gave their final approval to the manuscript.

Quantifying energy symbiosis of building-integrated agriculture in a Mediterranean rooftop greenhouse.

Joan Muñoz-Liesa*[1], Mohammad Royapoor[2], Elisa López-Capel[3], Eva Cuerva[4], Martí Rufí-Salís[5, 6], Santiago Gassó-Domingo[4], Alejandro Josa[1].

[1] Department of Civil and Environmental Engineering (DECA), School of Civil Engineering, Universitat Politècnica de Catalunya (UPC), Jordi Girona 1-3, Barcelona, Spain

[2] National Centre for Energy Systems Integration (CESI), Urban Sciences Building, Newcastle University Newcastle upon Tyne, NE4 5TG, UK

[3] School of Natural and Environmental Sciences, Newcastle University, Newcastle upon Tyne, UK

[4] Department of Project and Construction Engineering (EPC), Group of Construction Research and Innovation (GRIC), Universitat Politècnica de Catalunya (UPC), Edifici H, Av. Diagonal, 647, Barcelona, Spain

[5] Sostenipra Research Group (2017 SGR 1683), Institut de Ciència i Tecnologia Ambientals (MDM-2015-0552), Z Building, Universitat Autònoma de Barcelona (UAB), Campus UAB, 08193 Bellaterra, Barcelona, Spain

[6] Department of Chemical, Biological and Environmental Engineering, Universitat Autònoma de Barcelona (UAB), Campus UAB, 08193 Bellaterra, Barcelona, Spain

*Corresponding author.

Corresponding author email: joan.munoz.liesa@upc.edu, jmunozliesa@gmail.com.

Abbreviations

AHU	Air Handling Unit
ASHRAE	American Society of Heating, Refrigerating and Air-Conditioning
CV (RMSE)	Cumulative Variance of Round Mean Square Error
BIA	Building-Integrated Agriculture

CoP	Coefficient of Performance
ICTA	Institute of Environmental Science and Technology
iRTG	Integrated Rooftop Greenhouse
HVAC	Heating, Ventilation and Air Conditioning Engineers
MBE	Mean Bias Error
RTG	Rooftop Greenhouse
UAB	Universitat Autònoma de Barcelona
SCADA	Supervisory Control and Data Acquisition

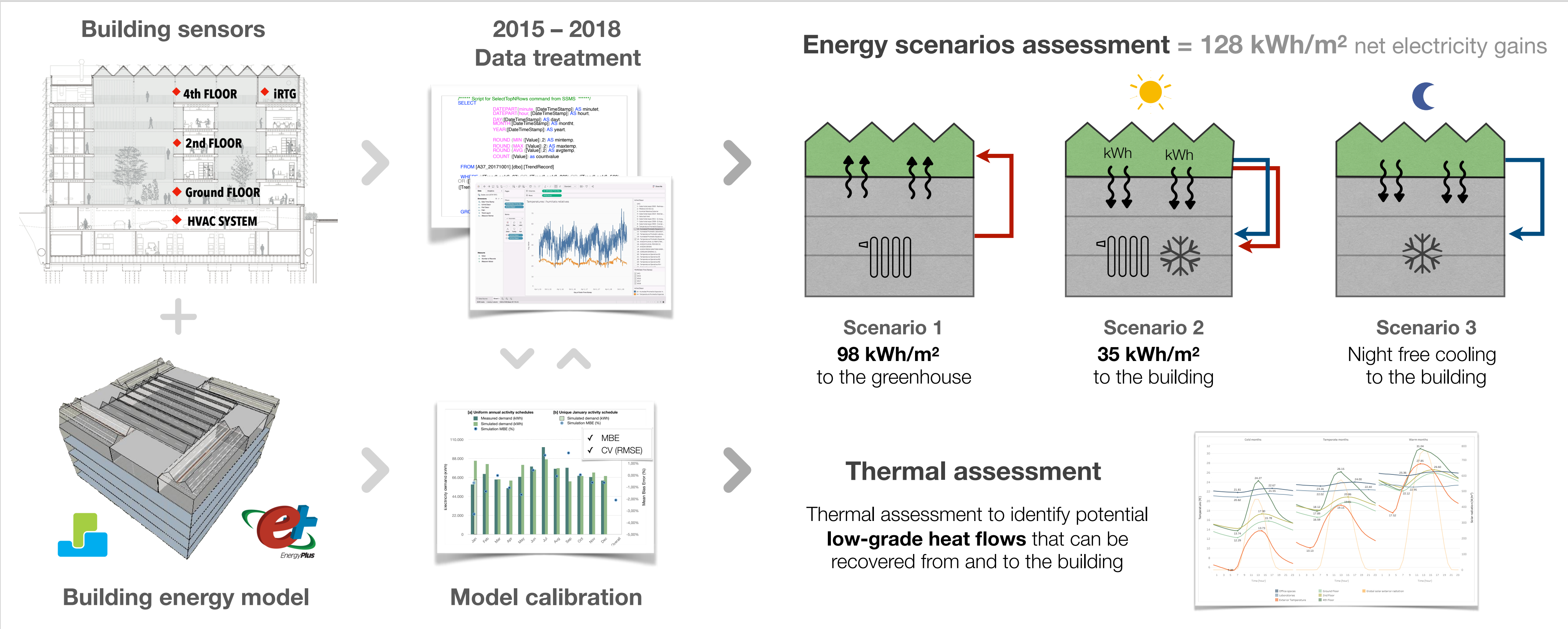

Building sensors
4th FLOOR
iRTG
2nd FLOOR
Ground FLOOR
HVAC SYSTEM
+
Building energy model
EnergyPlus
2015 – 2018
Data treatment
Model calibration
MBE
CV (RMSE)
Energy scenarios assessment = 128 kWh/m² net electricity gains
kWh
kWh
Scenario 1
98 kWh/m²
to the greenhouse
Scenario 2
35 kWh/m²
to the building
Scenario 3
Night free cooling
to the building
Thermal assessment
Thermal assessment to identify potential
low-grade heat flows that can be
recovered from and to the building

Quantifying energy symbiosis of building-integrated agriculture in a Mediterranean rooftop greenhouse.

Abstract:

A major concern for sustainable development is urban systems energy consumption. A possible way to gain additional whole system energy efficiencies is to integrate rooftop greenhouses (iRTG) on unoccupied roofs. This work presents actual environmental data (2015-2018) and calibrated energy modelling results to analyze the energy symbiosis between an iRTG and the host building. Simulation results illustrate that annually 98 kWh/m^2 of heating energy is passively recovered (84% during night time) from the building by the iRTG. Conversely the iRTG insulating capacity resulted in annual energy saving of 35 kWh/m^2 for the host building (equal to 4% of the building's annual energy needs). When combined an overall 128 kWh/m^2 of net energy savings and 45.6 kg CO_2 eq/m^2 of savings are realised via iRTG. On average, iRTG daytime temperatures can be 5.1ºC warmer (summer) and -4.3ºC cooler (winter) than the building. This presents major potentials for recovery and exchange of heating and cooling energy flows through integrating heating and ventilation air conditioning systems of the building and iRTG. Hence, iRTGs can provide a source of renewable energy as well as a sink for building exhaust air to improve energy efficiencies of urban built environment and urban agriculture.

Keywords

Energy modelling, energy efficiency, industrial ecology, industrial symbiosis, building integrated agriculture, urban agriculture.

Abbreviations

AHU	Air Handling Unit
ASHRAE	American Society of Heating, Refrigerating and Air-Conditioning
CV (RMSE)	Cumulative Variance of Round Mean Square Error
BIA	Building-Integrated Agriculture
CoP	Coefficient of Performance
ICTA	Institute of Environmental Science and Technology
iRTG	Integrated Rooftop Greenhouse
HVAC	Heating, Ventilation and Air Conditioning Engineers
MBE	Mean Bias Error
RTG	Rooftop Greenhouse
UAB	Universitat Autònoma de Barcelona
SCADA	Supervisory Control and Data Acquisition

1. Introduction

Energy-related carbon emissions are gaining increasing concern among societies [1,2] and represent a top priority for the international community to achieve a low-carbon future. Buildings account for 40% of the total energy consumption in Europe and produce 36% of the greenhouse gases [3]. More than 50% of dwellings date before 1970 and thus are not adapted to current thermal regulations[4]and are greatly energy inefficient. Also, only 0,8-1,2% of the building stock is renovated every year [5]; this is far from the building renovation rate of 3% suggested by the Energy Efficiency Directive [6] in order to reduce built-environment energy demand 32.5% by 2030. As a result, a wide range of global initiatives have the objective to increase building energy performance by legal mandates, policy instruments and directives in the EU [6-8] that encourage member states to apply energy efficiency measures in buildings.

Another currently inevitable trend is the 68% increase in urban population by 2050 with 85% of total population living in cities [9,10]. A direct impact is not only an increased demand and dependency on energy but also in water, food or land resources [11]. Moreover, these are normally shifted away from cities and thus, include the inefficient supply chains related to non-local resources. This is the case in agricultural systems, since the increasing population and the value of land in urban areas has moved food production away from urban regions, contributing to the increase in carbon-intensive supply food chains [12]. One of the most used agricultural systems for food production are greenhouses, as they efficiently use the resource-inputs to offer a controlled and resilient environment able to prolong crop season and improve crop yields [13-17]. Thus, they can potentially satisfy the growing demand [18]. In turn, however, they are the dominant energy consumers in the agricultural sector [19,20], accounting for 10-15% of the energy usage in Europe [21] and in developed countries [22].

Buildings and heated greenhouses are closely linked systems as they require high thermal and power demands during their respective operational phases [22,23]. In turn, both respective systems waste energy through (i) the building envelope (particularly when this is poorly insulated); and (ii) the greenhouse natural ventilation, when overheating occurs (>26ºC) at times of high solar irradiance. There are potential benefits from harvesting these wasted-energy flows by adapting an integrated and circular approach [24,25]. Low grade building waste energy can be used as a valuable heat input for greenhouses and vice versa in order to improve the sustainability of the combined system. This idea expands the prevailing systems approach that unites different isolated solutions to decarbonize multiple systems through the inclusion of other factors in a more holistic approach [26].

An illustration of current technologies and strategies that aim to improve isolated system elements are the studies that focused on reducing building energy needs by means of active (e.g., renewable energy) and passive solutions (e.g., insulation materials or bioclimatic strategies) [23,27,28]. Commercial greenhouses aim to reduce energy inputs also by active solar energy and ground heating solutions [29-31], and favor passive techniques such as north walls in east-west oriented greenhouses built at high latitudes in the northern hemisphere. These widely studied strategies [32] can save 30% of energy requirements [33], as they play an important role in greenhouse thermal insulation [34,35]. However, results from these studies show that they are not always sufficient, or that they should be implemented together with other solutions to progress into zero or nearly zero-emissions greenhouses and buildings [6]. To this effect, synergic approaches as building-integrated agriculture (BIA), demonstrate that industrial symbiosis has the potential to improve products and technologies by exploiting synergies with industrial neighbors through the exchange of materials and energy [36]. In turn, the development of industrial waste heat among other alternative heating systems, could reduce carbon emissions at the European level by 17–30% by 2050 with respect to the same heat demand level in 2010 [2].

The benefits of BIA have been studied from different perspectives, including food waste, nutrient and water cycle [37], to improve resource efficiency but not studied in depth from the energy perspective yet [38]. This is despite its benefits being commonly acknowledged widely [39-42]. Furthermore, existing rooftop agriculture studies focus on isolated energy benefits either from (i) the building perspective, due to the greenhouse insulation effect; or (ii) the greenhouse perspective, due to the energy gains recovered from the building. It could be because it requires integration and exchange of information between the various disciplines involved which need to solve more complex theoretical and practical issues [39].

From the greenhouse efficiency perspective, commercial greenhouses are identified as an ideal application for low grade industrial heat to produce food year-round [43]. In line with this, some studies have focused on energy savings derived from recovering low grade energy heat from both industrial parks [44,45] and buildings [12]. However, there are unexplored opportunities for capturing waste heat from adjacent buildings for non-rooftop agriculture as well [38]. Building's thermal storage media (i.e. concrete floors and brick walls) and its high thermal transmittance (approximately 0.9 W/m^{2}K) could offer plant-growing spaces that perform thermally better than most soils (equal to 0.5 to 0.8 W/m^{2}K, depending on the water content) [46]. In an integrated rooftop greenhouse (iRTG), the building's concrete rooftop absorbs solar incident radiation, converts it to latent heat during the day, and releases it at night inside the rooftop greenhouse [47]. Such iRTG industrial symbiosis have the potential to provide year-round growing conditions for food production in the urban context, as well as mitigate urban heat island effect [38].

From the building perspective, some studies demonstrate the energy savings derived from adding an insulation layer to a building through an iRTG [48-51]. Because of the limited number of studies conducted, these energy benefits are normally compared with other green infrastructures, such as green roofs, which achieve similar results [52-54]. Energy gains derived from evaporative cooling in greenhouses [55] have been explored, but very few studies address the potential benefits of reducing the HVAC building demand from utilization of greenhouse waste heat [51]. In this respect, rooftop greenhouses not only provide building energy savings by means of passive thermal insulation, but their climate controls can also be directly integrated into the building's HVAC system to exploit the energy savings of the overall system [38].

The aim of this work is to report the energy benefits of building integrated agriculture (BIA) by means of (i) a calibrated energy model and (ii) the thermal analysis of a case study building placed in a Mediterranean region that incorporates an integrated rooftop greenhouse (iRTG). This case study was previously assessed with a calibrated energy model that quantified the recovered heat from the building [12] and the greenhouse ([56]. Here, an improved version of this energy model is further analyzed and combined with additional real-world data from 2015 to 2018 to determine the thermo-physical influence of the iRTG on the building and vice versa. In doing so the overall net energy gains of the building-greenhouse system are presented, and guidelines to improve energy savings are given for three additional scenarios that are developed from observations of the case study building. This demonstrates the potential effectiveness of bidirectional energy symbiosis of building integrated greenhouses in order to improve the urban metabolism.

2. Methods

2.1 Case study

The Institute of Environmental Science and Technology (ICTA) is a research center and laboratory facility in the compounds of the Universitat Autònoma de Barcelona (UAB). The building is located in a suburban area in the Bellaterra Campus, Barcelona and is one of the first real-world demonstrator buildings that incorporates integrated rooftop greenhouses (iRTGs) in addition to the office and laboratory spaces. The building comprises of 2 underground floors (housing laboratories, building technical systems and parking facilities, see Figure 1 and Figure 2) and 4 more floors above the ground floor (housing the office spaces and laboratories on the 3rd floor). The fourth floor (i.e., the rooftop) integrates the 4 iRTGs (with two in operation, measuring 128 m^2 each) for food production and provides a research platform for building-integrated agriculture in the urban context. The translucent nature of the rooftop including the iRTGs constitutes a fundamental part of the building bioclimatic strategy and ecodesign, which also incorporates geothermal heat pumps and enhanced natural ventilation regimes via 4 atriums and a double skin façade. The geothermal heat pump (located in floor -1) actively heats the building spaces by means of the active floor, ceiling beams and air handling units (AHUs), which constitutes the heating and ventilation air conditioning (HVAC) system of the building. Every heated space in each façade hosts a machinery room where the HVAC system are located, including the AHU (see Figure 1 and Figure 2). These active heating systems are combined with passive strategies thanks to a Supervisory Control and Data Acquisition (SCADA) intelligent building automation system (see Table A.2 for component details), which enables automatic control adjustments and experimental data collection.

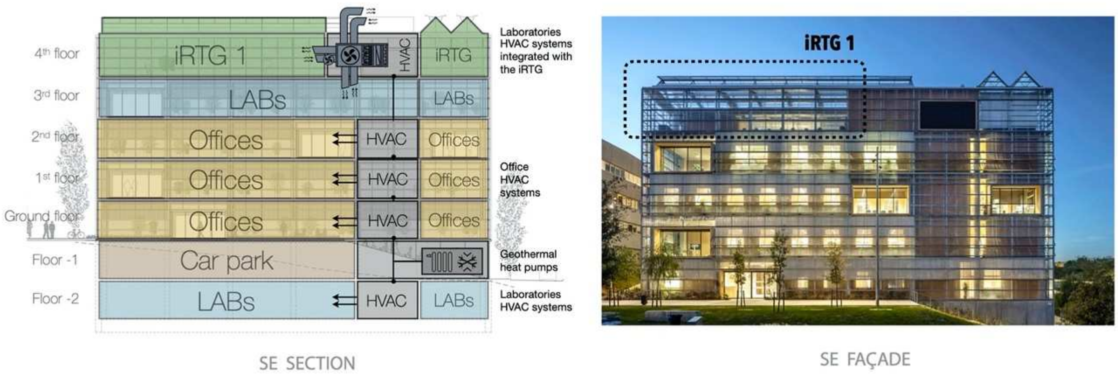

Figure 1. SE façade and cross section of the ICTA building and the iRTG 1 location in the 4th floor.

The integrated rooftop greenhouses are able to exchange resource and energy flows with the building by means of their shared physical space. To enhance this resource circularity, the AHUs and the HVAC control systems of the laboratories on the 3rd floor are located next to the iRTG (see Figure 1 and Figure 2); by means of inlet and outlet air pipes from and to the HVAC systems, exhaust air from laboratories can be conveyed to the greenhouses and vice versa when needed.

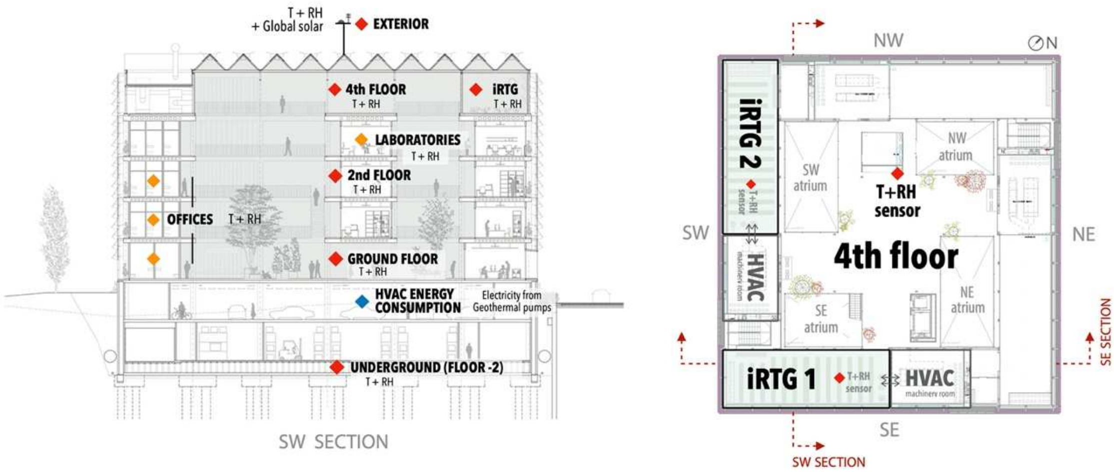

Figure 2. Temperature (T) and relative humidity (RH) sensors of the unheated common areas and exterior weather conditions (in red), heated offices and laboratories (in orange) and electricity energy meters from geothermal heat pumps (in blue) within the cross section of the ICTA building and floor plan of the 4th floor with the iRTG.

2.2 Climate control schedules and monitoring tools

The ICTA building is designed to satisfy both occupant and rooftop crop temperature requirements. Its climate is therefore actively managed leading to on-going control adjustments, either automatic (user defined) or manual (when needed, e.g., office window openings). The building has 3 season operating modes: winter mode from December to March; summer mode from June to September; and temperate months for the rest of the year. The ICTA building footprint is 40 m × 40 m and the building is 22 meters high. The translucent building envelope made out of polycarbonate supported by a steel structure forms the double skin façade and the rooftop fabric (see Table A.1). This volume contains an interconnected unheated volume that houses different isolated heated spaces inside. These heated spaces are climatically controlled according to their usage, leading to 5 control schedules that administrate their internal climate as follows:

1. Workspaces and offices are kept at of 21-23-25ºC depending on the season (winter – temperate – summer). Users can regulate these temperatures ± 1.5 ºC if desired.
2. Laboratories (at 3rd floor and floor -2) range from 22º to 23ºC depending on the laboratory requirements. At the 3rd floor, continuous air extraction from 7:30h to 20:30h maintains the laboratory equipment at a differential positive air pressures of +10 Pa.
3. iRTGs (4th floor) are not actively heated. When available and according to building air renovations, forced ventilation from laboratories can passively heat or cool the greenhouse (see Table A.2 for detailed specifications). Thermal-shading curtains (see Table A.1) can isolate the greenhouse spaces with the building and the exterior when needed. Automatic window openings of the rooftop and the façade of each iRTG are independently controlled with respect to the rest of the building skin. The greenhouse internal temperature defines the opening angle of the side windows on the roof and the façade starting at 22ºC (10º opening) to 27ºC (45º opening, with 3 minutes of system-defined dead band).
4. Open common space areas are not actively heated or cooled. The inner temperature of the unheated common areas are calculated by the average of the sensors placed in the ground, 2nd and 4th floor (Figure 2). This average temperature determines when the rooftop windows automatically open to naturally ventilate in case of overheating (i.e. independently from the exterior temperature). The system-defined temperatures are set at 30 ºC, 24 ºC and 22 ºC during winter, temperate and summer months respectively with a -3ºC

dead band. Rooftop-automatic windows also open when temperatures in the rooftop reach 28ºC on all seasons.

5. Double skin façade. Analogously to the rooftop operating system, temperature sensors placed in the midpoint of each double skin façade (and in ground, 2nd and 4th floors) are used to calculate the average of each double skin façade temperature. These determine the target temperatures that automatically open one-side windows in each building skin façade at 26 – 24 – 22 ºC with -4ºC of dead band, according to season.

The SCADA control panel comprises the main building automation system responsible for the working modes, climate controls, windows schedules, etc. The interface is provided by Desigo™ Insight software (Siemens Building Technologies Ltd) and integrates all building sensors (> 2000) and actuators. Part of these components (340) produce hourly data, measuring temperature and relative humidity (Siemens Symaro QFA3160 with an accuracy of ±0.6ºC and ±2% respectively), and energy (Siemens Sentron PAC3100, with an accuracy standard Class 1) that is recorded in a SQL database since September 2014. Data error checking and depuration process are latter performed with Tableau Desktop (Tableau Software). These tools are offered to the building operators and researchers in order to monitor, check and control the operating system in a coordinated way.

In order to prevent data losses and check the sensors accuracy, 85 sensors from a Campbell data acquisition system complements the Siemens building data. Sensors placed in the iRTGs and inside and outside the building measure the air temperature (Campbell 107, ±0.18ºC accuracy) relative humidity (Campbell CS215, ±2% accuracy) and global solar radiation (Hukseflux LP02, second class pyranometer) every 5sec, recording the averages at 10-minute intervals. Figure 2 shows the location of the main sensors used to report the results of this work from Siemens and Campbell systems.

2.3 Data backhaul and model calibration

The availability and affordability of pervasive sensors and energy consumption data in the ICTA building (and the wider building industry) has enabled the creation of high-fidelity energy models that have the potential to improve environmental strategies, aid the design of advanced control strategies [57] and optimize building materials and retrofit solutions [58]. When calibrated to meet American Society of Heating, Refrigerating and Air-Conditioning Engineers (ASHRAE) Guideline 14 [59] acceptance criteria, EnergyPlus models have been demonstrated to predict 99.5% of annual hourly temperatures with an accuracy of ±1.5 °C [60].

A vast volume of information is required to adequately describe a building which nonetheless contain major simplifications within the modeling work. Given that the research team intended to assess both energy and environmental performance of building integrated agriculture in the ICTA building, an EnergyPlus model was devel0ped and calibrated using both building energy and iRTG internal zone dry-bulb temperature and relative humidity. An earlier publication reported on the prediction accuracy of the EnergyPlus model that reproduced annual internal temperature and humidity results with respective MBE and CV(RMSE) values of 2.6% and 11.5% (RH) and 2.9% and 15.9% (temperature) [12]. In order to examine additional energy scenarios in this work, new calibration results are reported using the aforementioned EnergyPlus model that are parameterized with thermo-physical and operational parameter inputs outlined in table A1. Metered monthly energy consumption belonging to year 2015 and site-specific weather data (direct and diffused solar irradiance (Wh/m^2), temperature and relative humidity, wind speed and direction, atmospheric pressure) are used within an EnergyPlus v9.2 platform. As well as modelling data, actual high-resolution field data from years 2016 to 2018 compiled using building management sensors has been used to report on the thermal benefits of rooftop greenhouse integration and build evidence on all energy saving potentials. Finally, by combining modelling and real data, several energy related alternative scenarios are proposed and investigated in order to offer insight scaling the learning from ICTA building across other climatic conditions.

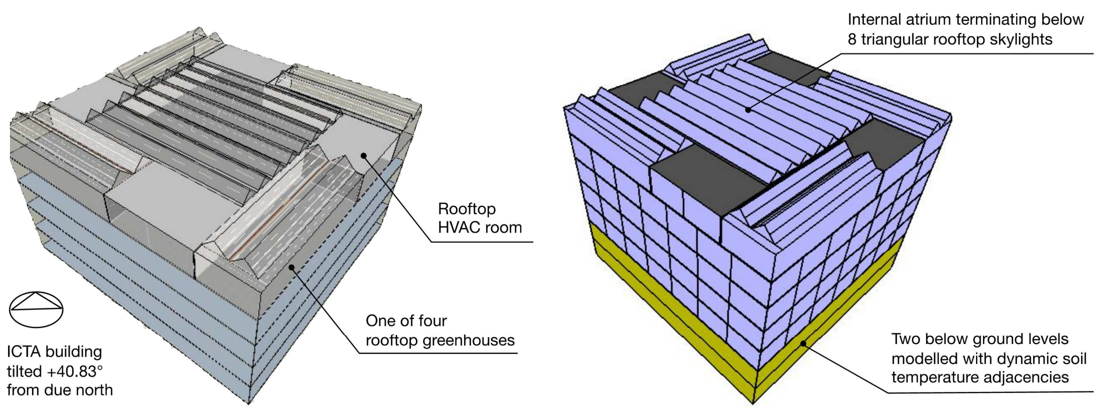

Figure 3. Rendered global view of calibrated EnergyPlus model with four iRTG configuration outlined.

More specific to the nature of modeling effort in this work is the deployment of EnergyPlus Energy Management System to introduce dynamic cooling effect of plants in the greenhouse. This experimental solar-radiation based model for Mediterranean greenhouses developed by Bonnachela [61] has been used as a control logic in EnergyPlus to compute plant transpiration and cooling effect. This is to reflect significant coverage of dense vegetation in summer months (for tomato crop cycles from January to July) that produces a cooling effect through plant transpiration as opposed to a conventional roof surfaces that absorbs and transmit solar energy into the building. Additional details on optical properties of translucent material, surface convective coefficient representation and plant transpirations are available in [12,56].

2.4 Energy scenarios

In order to assess the energy benefits from the building to the greenhouse and vice versa, three scenarios are proposed (Figure 4). These additional scenarios aim to identify and assess separate possible energy-flow paths across hourly and monthly conditions through all year. The scenarios presented here are all passive and require no additional energy inputs, but offer exchange of existing energy flows that improves overall efficincy as identified in established classifications [15]. Each scenario can include multiple energy flows, numbered and cited accordingly. The energy assessment of scenarios 1 and 2 has been done through calibrated EnergyPlus models (using 2015 data for calibration) which simulates year 2015 climate conditions, while scenario 3 has been supported with the hourly temperature records available from 2016-2018 period. The results assess the overall benefits of the energy symbiosis of the integrated systems under examination here.

- Scenario 1 evaluates the heat flows transferred from the building to the greenhouse through calculating the energy demand of an identical greenhouse model in a freestanding condition placed on the ground. For that purpose, a complete model of the iRTG and the ICTA building was previously calibrated to validate building and greenhouse model performance [12]. Next, a virtual model of the iRTG detached from the building was simulated maintaining the same geometry and corrugated polycarbonate covering (U-value = 5.7 W/m^2, see table A.1) operated in a freestanding mode in the same location and under the same operating regime as the iRTG in the ICTA building (i.e. window openings, operating schedules and occupancy pattern). The heating benefits (kWh/m^2) of the iRTG can be obtained by simulating the freestanding model to achieve the same inner temperatures as the integrated greenhouse. In doing so the heating system in the freestanding greenhouse model simulates the same thermal demand as was recovered in the form of waste heat from the building by actual iRTG. Actual 2015 zone air temperature in iRTG form EnergyPlus target temperature for the freestanding model to accurately replicate the iRTG internal environmental conditions, while KIVA software 0.3 generated hourly soil temperatures for the freestanding greenhouse model to account for zone air to soil thermal interactions in the freestanding model. Here, further analysis in this energy model allowed to identify night and day heating requirements and properly contextualize the resulted benefits with the energy and thermal assessment of the building.

- Scenario 2 evaluates the insulative effect of the greenhouse for the building through calculating the heating demand of the building without the iRTGs on rooftop level. To this purpose, the calibrated model of the ICTA building with the iRTG has been modified by removing the polycarbonate translucent rooftop (U-value = 5.7 W/m^2, see full description on table A.1). The resulting new roof on the 3rd floor is defined with a standard light-weight concrete roof structure insulated with an extruded polystyrene and concrete finishing layers that achieves a U-Value of 0.41 W/m^2K, according to the minimum thermal requirements outlined by the Spanish Technical Building Code for the Barcelona region CTE-DB-HE [62].

- Scenario 3 investigates the night cooling effect of the building envelope through the automatic windows of the ICTA building and the iRTG by analyzing the hourly temperatures registered within the unheated spaces of the building. The rooftop windows operate as a Venlo greenhouse, with openable roof windows on both sides of the ridge. Currently these windows open automatically up to 45º respect to the roof slope (also at 45º from the horizontal plane, see Figure 1 and Figure 2). However, during nighttime, they open for a maximum angle of 15º only to avoid water condensation when the mean temperature of the building rises more than 22ºC while maintaining a -3ºC of dead band (as mentioned in section 2.2). The exterior climate therefore influences the temperature drop in the 4th floor to provide cooling benefits to the rest of the building as evidenced by observing actual temperatures resulting from this night cooling strategy.

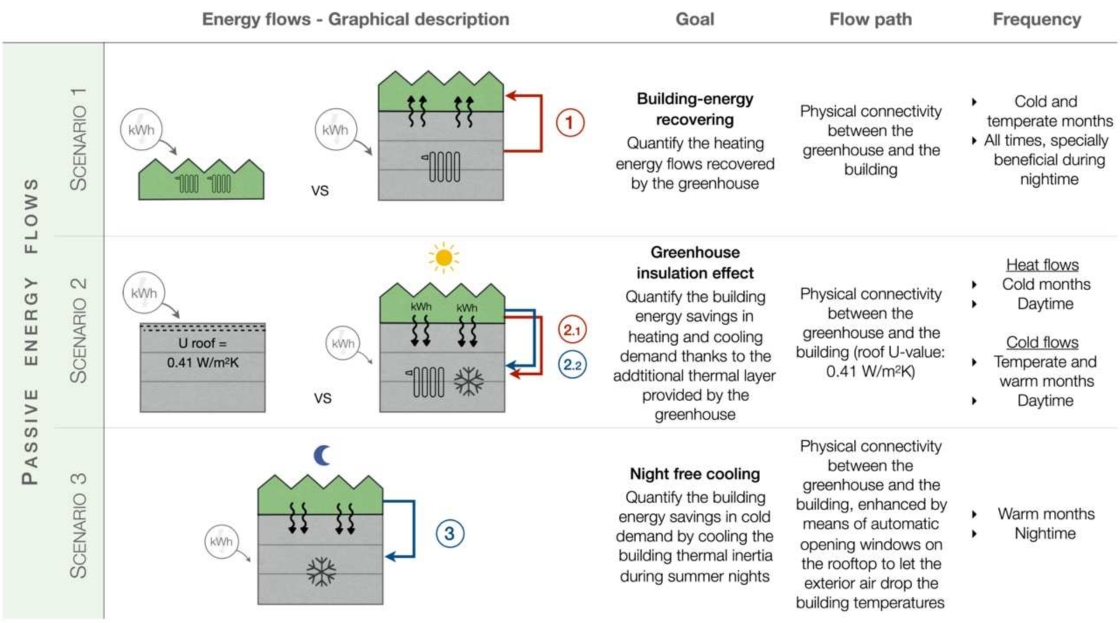

Figure 4. Studied energy scenarios with each scenario goal and detailed energy flows properties.

3. Results and Discussion

3.1 Calibration results

As noted earlier, calibrated models – when parameterized with detailed thermo-physical and operational building characteristics – have been demonstrated to produce environmental and energy predictions with minimal errors. The energy model was calibrated with actual site-specific hourly temperature, relative humidity, wind and solar irradiance data from 2015 [12]. The simulation results presented here has been built on previous work [12,56] whereby through a systematic version control method, 25 successive model versions were refined progressively to produce monthly Mean Bias Error (MBE) and Cumulative Variance of Round Mean Square Error (CV (RMSE)) values for model electricity prediction using expressions 1 and 2:

$$MBE = \frac{\sum_{i=1}^{N_i}(M_i - S_i)}{\sum_{i=1}^{N_i} M_i} \quad (1)$$

$$CV\ (RMSE) = \frac{\sqrt{\sum_{i=1}^{N_i}[(M_i - S_i)^2/N_i]}}{\frac{1}{N_i}\sum_{i=1}^{N_i} M_i} \quad (2)$$

where M_i and S_i are respective measured and simulated energy data at month i, and N_i are the 12 months used to calculate error against 2015 actual data. The main indices for the parameterization of the model are outlined in Table A.1. Most notably given that heating and cooling in the case-study building is provided by GSHPs, coefficient of performance of these units were set to 3.5 (heating) and 2.5 (cooling mode) in order to reflect the real world findings outlined in Table 3 of [63]. These energy calibration results are illustrated in Figure 5 [a]. As evident, the

EnergyPlus model creates its largest errors (a MBE of -3.3%) in the month of January. While all across the year the HVAC and activity schedules governing EnergyPlus simulation of ICTA were kept constant, a reduced activity schedule for the month of January alone had to be defined in order to reflect the more limited amount of occupant's activity in January in order to finally arrive at the calibrated model energy MBE and CV(RMSE) values of -2.1% and 12.7% respectively. Both of these indices fall within the ASHRAE guide 14 calibration limits [59].

Despite achieving compliance figures, under -predictions persist in summer months (July and September) due to natural ventilation from stochastically occurring manual window opening and such stochastic activities are not captured by the deterministic schedules overseeing the EnergyPlus simulation. While model energy results achieve calibration criteria, the more random nature of reality is evident in the final results presented here. The final calibrated model produces an overall annual over-prediction of 17.7kWh (or -2.1%) with maximum and minimum monthly errors occurring in September (+1.8%) and October (+0.03%) respectively. Further work could also more closely match acceptance criteria for electricity consumption values across multiple years as well as investigate the accuracy of model temperature and humidity predictions.

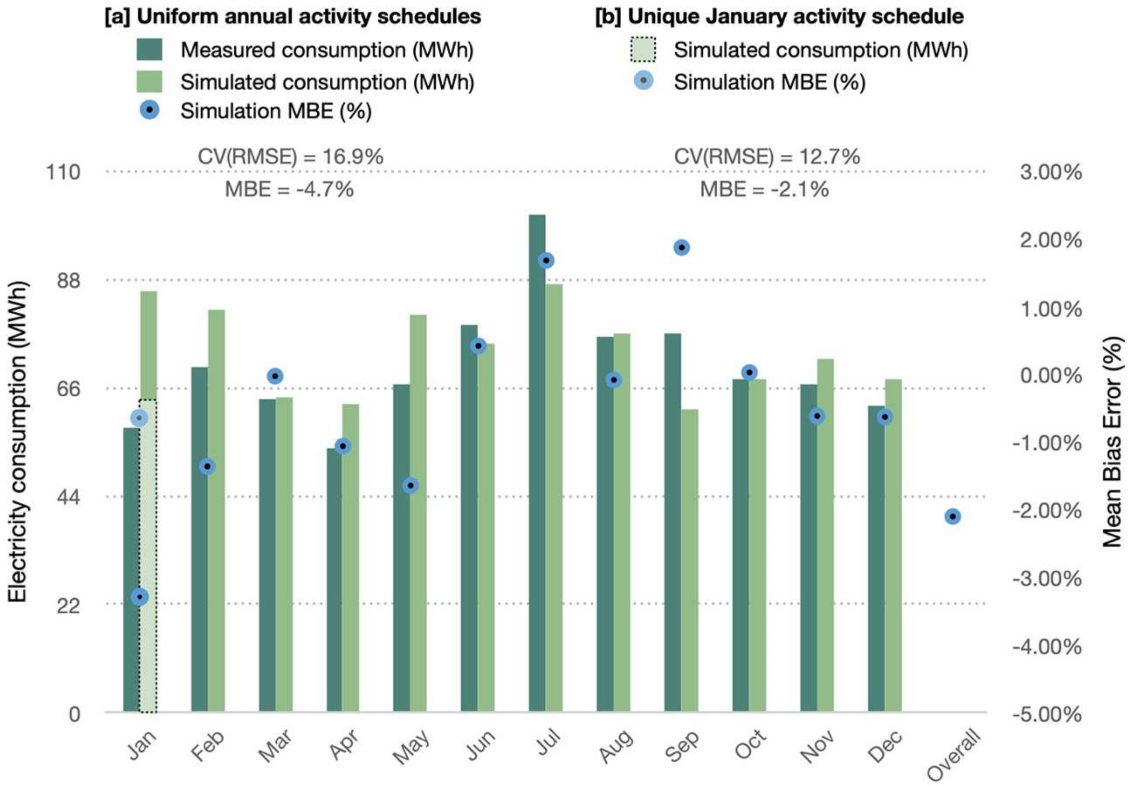

Figure 5. Calibration results for E+ model with 2015 measured demand and simulated demand with [a] Uniform annual activity schedules and [b] Unique January activity schedule.

3.2 Building thermal performance

Average building hourly temperatures, including unheated and uncooled zones, were recorded during 2016 to 2018 period (Figure 6). For each month, the average hourly measured air temperature of the ground, second and fourth floors are represented as shown in the x-axis (see Figure 2). These air temperatures capture the condition of the unheated zones of the ICTA building which are located between office and laboratory spaces (for ground to 3rd floor) and also between the iRTGs on the 4th floor. Broadly speaking the graph shows a high stratigraphic temperature distribution within the building floors. These thermal gradients are strongly influenced by the building materials that act as a thermal stabilizer across the whole year in the ground and second floor (hourly temperatures vary from 3 to

5ºC daily), with the second floor being always warmer than the ground floor. Conversely, the greenhouse effect dominates the 4th floor temperatures during day due to the translucent greenhouse cover. Thus, hourly average temperatures are more dynamic across the year, and more similar to the exterior temperature during night time, when they are influenced only by the concrete slab and the building inertia

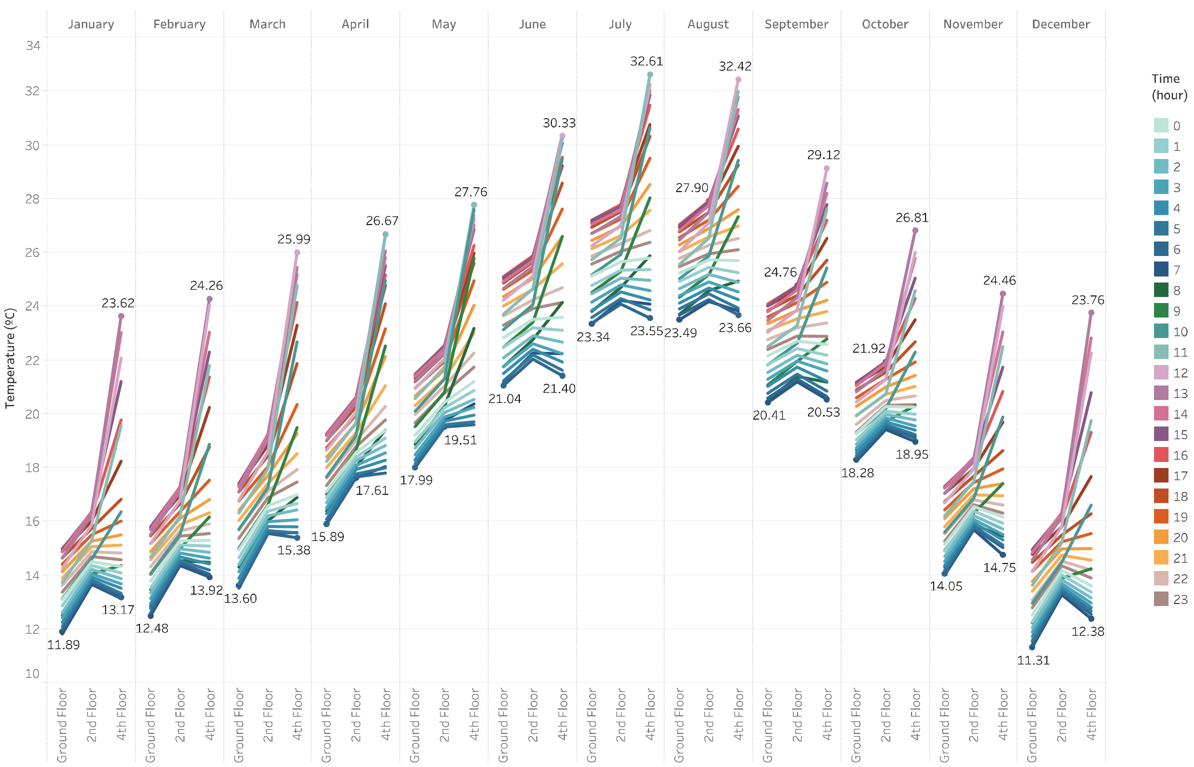

Figure 6. Monthly and hourly (in color scale) average temperatures recorded during the 2016-2018 period on the ground, second and fourth floor of the ICTA building.

The wide range of hourly average temperatures across the year allow us to understand the overall thermal distribution within the building including the rooftop (Figure 6) and building heated areas (Figure 7). This wide range of thermal profiles within the envelope of the building highlights the potential energy gains that can be exchanged between most appropriate spaces. In order to condense a large number of data points and enable insights to be derived, the analysis here focuses on three seasonal variations, namely (i) cold, (ii) hot and (iii) temperate months.

(i) During the coldest months (from December to March), minimum ground floor temperatures were 11ºC at 7h, and raised to a maximum temperature of 17ºC at 15h. Similarly, temperatures ranged from 13 to 19ºC on the second floor. These common areas are not actively heated but still reach 14ºC during most of the annual cycle (91% of hours), which is within the human comfort temperature for transit areas [64]. By contrast, temperatures inside the iRTG on the 4th floor are more dynamic than ground and second floor temperatures, with temperatures ranging from 16 – 26ºC during daytime and 14 to 18ºC at nighttime, which generally satisfy the optimal temperatures for crop cultivation.

(ii) During the hottest months (June to September), there is a wider range of temperatures in the ground and the second floor of the building than in cold season, with temperatures ranging from 21 to 27ºC. The greenhouse is cooler between 7 and 9h in the morning than between 12 and 13h, when it reaches maximum temperatures of 31ºC (see Figure 6). Maximum greenhouse temperatures of 31ºC have a negative effect on plant growth (optimum crop growth temperatures is 13-20ºC at night and 20-28ºC during day time, depending on crop types) [65]. The building thermal inertia created by 48 cm lightweight concrete slab floor system (which incorporated circular service ducts) negatively effects ideal night temperatures for crops as they are greater than 20ºC (see Figure *7*). The exposed rooftop floor to the exterior night conditions produce greenhouse temperatures 0.5ºC lower than temperatures in lower building floors. Cold temperatures are transferred to the concrete media and produce thermal inversion in the rooftop, aiding to cool down greenhouse daytime temperatures from 7 to 9h. Furthermore, the opening of iRTG and automatic building façade windows and high wind speed on the rooftop provide natural ventilation. Wind velocities on the rooftop are 2.6 times higher than at 2m above ground floor. Wind velocities are also higher during the hottest periods of the day (14-17h), enabling more passive ventilation and therefore building cooling capacity to overcome the rising temperatures in the greenhouse.

(iii) Finally, during temperate months (April, May, October and November) intermediate temperature conditions between the hottest and coldest months are recorded. Minimum temperatures are around 14 to 18ºC while rooftop greenhouse temperatures rise to nearly 28ºC. This excess of temperatures in the rooftop combined with low temperatures in the communal spaces offer an ideal condition to recover and convey waste heat from to greenhouse to the building and store it by means of its thermal mass.

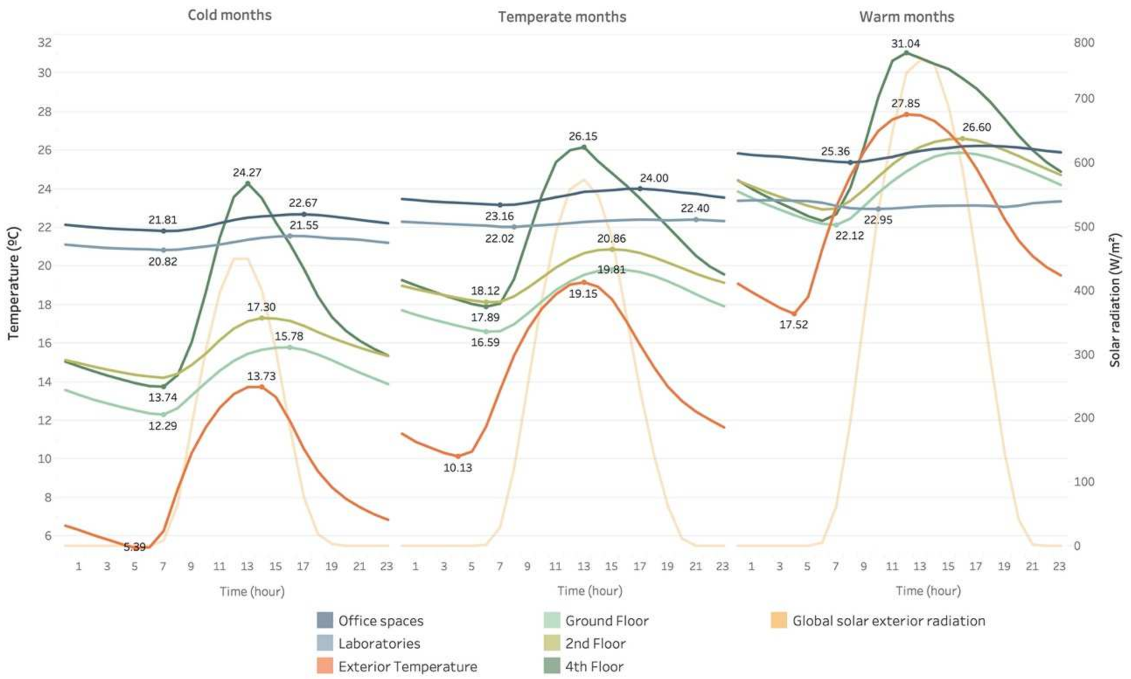

Figure 7. Hourly average temperatures within the ICTA building and exterior global solar radiation in cold, temperate and warm months

3.3 Thermal energy potential

As illustrated in Figure 7, the temperature dynamics of exterior and unheated building spaces have a notable contrast with more constant environments of offices and laboratories that are actively heated at temperatures between 21 and 25ºC. Also, the building high inertia forces the building HVAC system to be permanently operating, offering the possibility to heat and cool the greenhouse all over the year thanks to the system integration with the greenhouse. Thus, office air exchange and exhaust air from laboratories can be redirected to the greenhouse instead of discharged to outside, aiding to heat and cool the greenhouse. Night time thermal differences between offices versus greenhouse spaces are respectively 5.7 ± 2.4ºC (cold months) and 3.6 ± 1.5ºC (temperate months) which present a potential source of heat for the greenhouse. Laboratories also offer cooling capacity, especially during warm months given that they are 4.3 ± 2.7ºC cooler than rooftop spaces.

The greenhouse can also heat the building by acting as a solar collector [66]. The rooftop temperature reached more than 21°C during 73% of the annual daytime (or 53% of the total annual hours) across the observational horizon of 2016-2018. Also note that in January, temperatures reached up to 24ºC, which translated into a +10.6ºC difference with respect to exterior temperatures during peak sun hours. Minor differences occurred during temperate (+7.0ºC) and warm months (+3.2ºC) as the excess of heat is then dissipated thanks to the automatic building natural ventilation. The closed greenhouse concept [67] can be applied to convey the excess thermal heat (i.e., when available) to the building with forced energy flows that could maintain the greenhouse temperature while reducing the building energy loads. Further research could capture this active intra-building energy exchange scenarios to explore all possible energy flow exchanges between the building and the greenhouse.

3.4 Energy scenarios

Scenario 1: Building energy recovery: The building waste heat recovered by the greenhouse has been estimated in this scenario by simulating the heating energy needs of a freestanding greenhouse. These energy benefits were modelled in previous work [12] which using 2015 site-specific weather data equated to 342 kWh/m^2/year of thermal energy. This work showed that maintaining the same environment as iRTG in a freestanding greenhouse resulted in monthly energy needs that were highest during night time (288 kWh/m^2/year, i.e., 84% of annual energy needs), and especially during winter time when average night temperature range was 4 – 8ºC (Figure 8). This can be explained through the temperature drops registered during night time in the 4th floor compared to other building floors (Figure 7), which denotes heat energy flows are being transferred from the building to the greenhouse. Hence, the iRTG specially benefits from the building inertia during nighttime, when iRTG temperatures compared to the exterior can be up to 8ºC higher during cold months. Nighttime benefits are also reported in other greenhouses in the BIA context [68]. Similarly, heating requirements are lower as average temperatures increase. However, note that there are daily heating needs even in summer months in early morning hours [12]. The overall annual greenhouse simulated heating load is in line with the average heating load demand of 416 kWh/m^2/year for north-west European countries [69] and in the Mediterranean region, within 139-444 kWh/m^2/year [12]. Finally, if these heating needs were covered by the same building ground source heat pumps (CoP 3.5, see Table A.1), the equivalent electricity needs would be 98 kWh/m^2. This allows to compare simulation results between scenarios while considering the electricity inputs to passively operate the greenhouse.

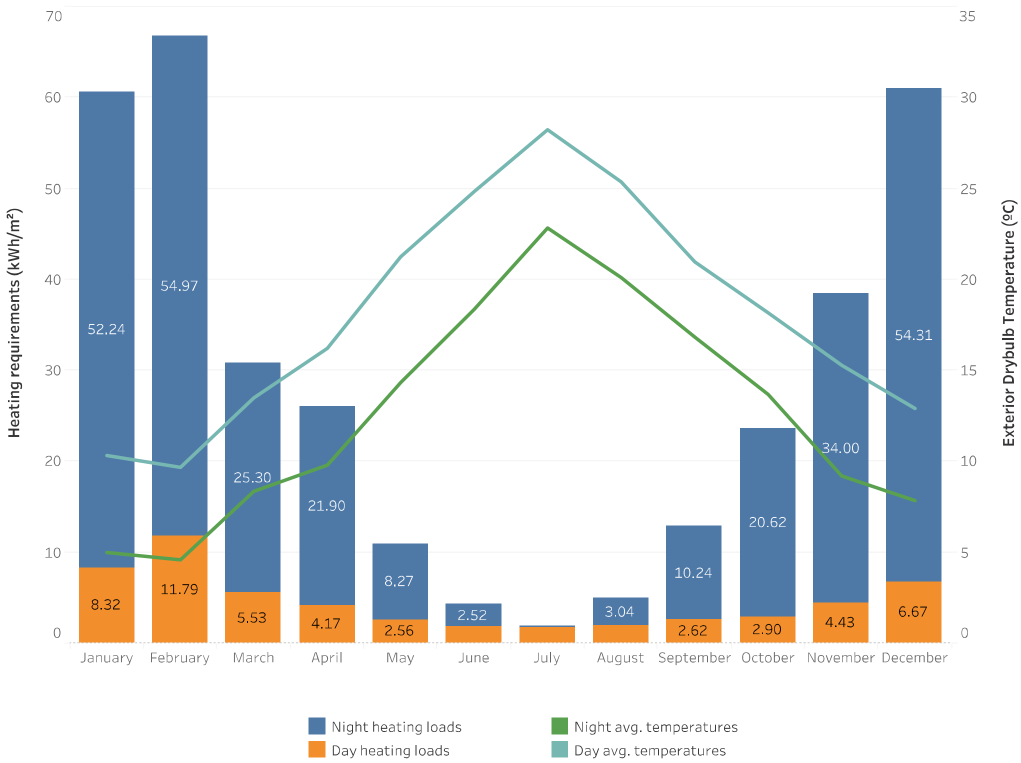

Figure 8. Monthly energy needs of the freestanding greenhouse during day and night time (left axis) with average day and night time dry bulb temperatures (right axis).

Scenario 2: Greenhouse insulation effect: Rooftop greenhouses have positive effects on the building thermal insulation [15,39,70] similarly to other building green infrastructure types [71-73], including living walls [53,74]. In this work, EnergyPlus simulation results showed a 32 kWh/m^2/year (expressed as m^2 of greenhouse) of net reduction in the building electricity consumption that is used for space heating. Moreover, this is noticeable in cold months and particularly from October to April in 2015 (see Figure 9) when the rooftop temperature is higher than the building temperature. The buffering effect in the greenhouse acts as a passive insulative layer for the building during daylight time. Therefore, the space heating produced by solar irradiance and realised in iRTG is beneficial not only for the crop environment in iRTG but also the host building. During the hottest periods when higher solar irradiance is available for plant growth, more biomass will also be available that could block solar radiation with plant leaves. That will reduce the sunlight reaching the rooftop and hence, reduce overheating. Evapotranspiration effect of plants produces a cooling effect [74] in the same way as the evaporative cooling works in greenhouses [55], which is currently used as a passive technique to reduce the overheating in building-integrated agriculture [75,76]. Due to this effect and the greenhouse insulation capacity all over the year, simulation results point that evapotranspiration of plants supersedes the greenhouse effect and show a small reduction of the building net cooling duty of 3 kWh/m^2/year. However, there have been overheating hours in the inner spaces between greenhouses (were plants are not grown) with temperatures reaching up to 32ºC and this could imply that additional cooling is needed for the rest of the building if the greenhouse surfaces are not covered by plant foliage and merits further analysis.

The overall net insulation effect of the iRTG sums up to 35 kWh/m^2/year and represents 4% of energy savings on the annual building electricity needs. This result is in line with previous studies quantifying the energy savings from adding an iRTG to a building as an insulation layer [48-51]. These studies have shown that, depending on the roof insulation capacity the energy savings can range from 3 to 13% of building demand. Here, the insulation capacity chosen is 0.41 W/m^{2}K to represent fabric thermal requirements defined by the Spanish Technical Building Code [62]. Thus, considering the poorly insulated building stock in Europe, greater energy savings can be obtained by adding rooftop greenhouses as a retrofit measure in buildings [48].

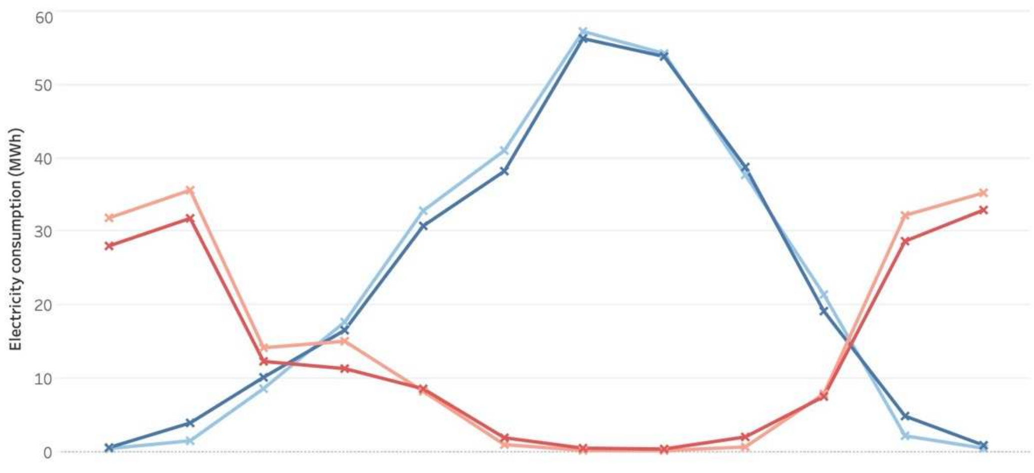

	Jan	Feb	Mar	Apr	May	Jun	Jul	Aug	Sep	Oct	Nov	Dec
Qh I+iRTG	28.03	31.79	12.31	11.33	8.58	1.92	0.50	0.39	2.03	7.53	28.68	32.92
Qh ICTA	31.85	35.62	14.17	15.06	8.24	0.99	0.20	0.17	0.66	7.89	32.19	35.26
Qc I+iRTG	0.58	3.94	10.14	16.55	30.76	38.21	56.26	53.82	38.77	19.15	4.87	0.90
Qc ICTA	0.44	1.51	8.61	17.67	32.83	41.02	57.23	54.23	37.70	21.41	2.18	0.48

Figure 9. Simulated monthly heating and cooling electricity consumption (MWh) during 2015 for ICTA building with and without iRTG (scenario 2).

Scenario 3: Night time free cooling: It is possible to provide night time cooling for the building during warm months (from June to September) due to the lower temperatures recorded in the rooftop that aid to cool down the building carcass overnight (Figure 7). This scenario is advantageous and works under a very simple principle: the automatic opening of rooftop windows that introduces the cold exterior air into the building, lowering down the temperatures of air and building mass. Colder air masses are naturally displaced through the rooftop and the atriums to the rest of the building, including inside office spaces equipped also with automatic windows. This produces a notable signature in the actual recorded temperatures as there are higher night time temperature drops in the ground and 2nd floors during warm and temperate months compared to cold months (Figure 7). This night time cooling capability also takes advantage of an existing iRTG asset when considering the greenhouse as built by default and without additional running costs.

Night free cooling also produces thermal inversion to the rooftop level zone as exterior temperatures are higher from 7 to 9h in warm months (Figure 7). This occurs as the rooftop structure emits more thermal radiation than it receives from the exterior, which cools down the building and the excessive summer temperatures registered in the greenhouse (see section 3.2). This is a common phenomenon reported in unheated conventional greenhouses [77] which in the case of an integrated greenhouse has the added benefits of cooling down the building as well as iRTG.

Ultimately, cooling effect obtained in the rooftop and transferred to the building can be seen with lower temperatures being recorded on 4th floor compared to the 2nd floor from 1 to 7h. From August to September, 4th floor temperatures can be lower than those recorded even in the ground floor. This is a particular feature of the ICTA building which is enhanced by its atriums, façade envelope and building design. Similar advantages would be achieved in other forms of translucent rooftop envelops (e.g., colonnades, between buildings, covering the inner spaces between façades, forming galleries).

3.5 Whole system energy performance and recommendations to improve energy benefits

Energy-scenarios assessment quantified the energy benefits and drawbacks of building-integrated agriculture in the ICTA building. The greenhouse recovered an equivalent annual electricity of 98 kWh/m^2 when heated with the same building HVAC system, and the building net gains were 35 kWh/m^2 (see Figure 10). However, additional electricity inputs are needed to operate the automated building system which integrates a server with programmable logic controllers attached to sensors and actuators (i.e., windows and curtains). This system manages the building passive energy strategies to enable the building and the greenhouse to interact energetically with the exterior. Similar to sensor data, the building SQL database also records the actuators' operation, enabling the calculation of total energy inputs. During 2015, 5 kWh/m^2 were necessary to manage the building passive climate (mostly due to the Siemens servers, see Table A.2 for further details), leading to a net energy balance of 128 kWh/m^2. Considering the Spanish electricity mix for low voltage (Ecoinvent 3.5 [78]), an equivalent carbon and cost savings of 45.6 kg CO_2 eq/m^2 and 15.1 €/m^2 would be obtained (reflecting 2015 building electricity costs). Further energy modelling analysis could also integrate the night cooling effect in equivalent electricity loads. Moreover, additional passive strategies (such as the thermal curtains operating in the 4 iRTGs but not in the entire 4th floor) could also be applied and modelled to maximize the BIA benefits.

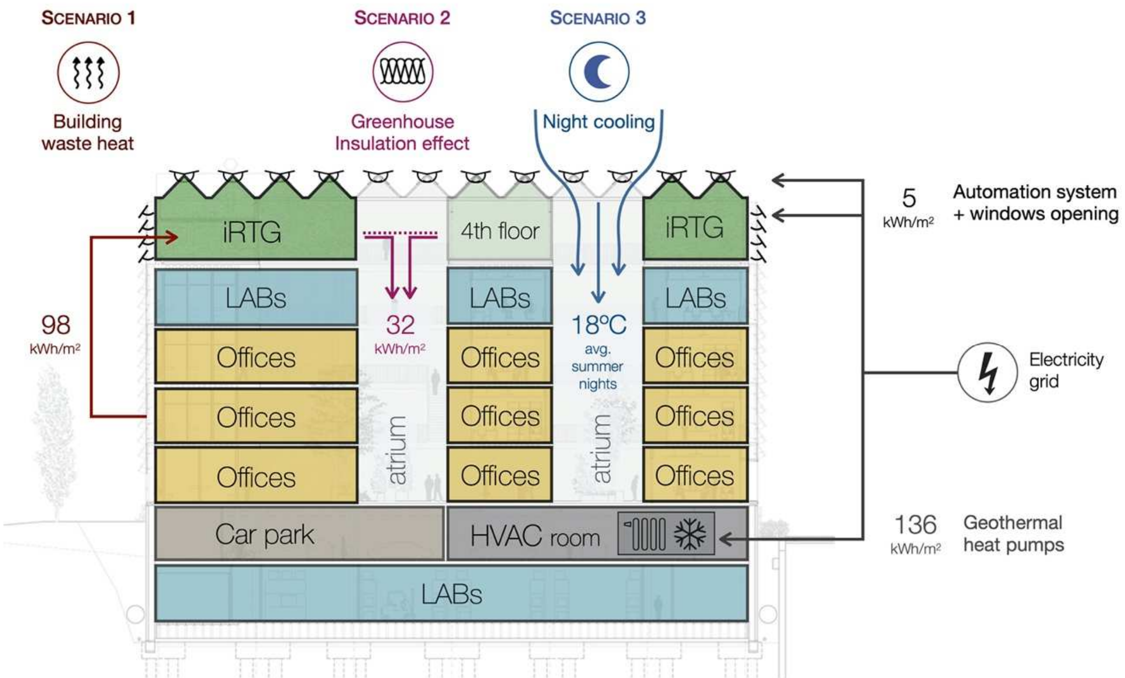

Figure 10. Overall system energy performance.

In *scenario 1*, the temperature drops in the rooftop also produce heat energy losses during night time and cold months, cooling down the rest of the building. Even larger benefits during day time overcome these energy loses (see Figure 9). Increased energy benefits can also derive from improving the 4th floor insulation by means of roof and wall thermal curtains, which can overcome this effect increasing night temperatures up to 2.4ºC in unheated greenhouses [77]. During the coldest months, they also prevent thermal inversion which is frequent in Mediterranean areas and are a clear advantage compared to conventional greenhouses [77]. Between 20-50% of energy savings were also reported in heated greenhouses, which results in less than three years of payback [47]. Thermal-energy curtains are also a common environmental-energy feature in building rooftop greenhouses such as Lufa Farms in Montreal, Canada [79,80] and thus represents a potential benefit that should be considered in the ICTA building in future studies.

In *scenario 2*, roof thermal screens are a common passive solution in Mediterranean greenhouses in order to block excessive solar gain in peak hours and prevent overheating [81]. However, automatic screens tested in the ICTA building also notably decrease roof natural ventilation and around 60% of the incident radiation for greenhouse crops. Thus, there is an optimum point of curtain opening considering building needs, crop irradiation necessities (that saturates leaf net photosynthetic rate [82]) and thermal performance of the greenhouse-building system. However, in 4^{th} floor common area, thermal curtains would improve peak temperatures over 30ºC registered during summer months. However, a trade-off should be also done considering that thermal curtains will also block office natural light.

In *scenario 3*, larger benefits could also be achieved in the ICTA building by improving the operating system of the automatic windows in the rooftop, for instance by allowing 100% of window opening capacity before 22ºC is reached. Hence, enhancing better natural ventilation during summer nights to better cool down the building temperatures. The 5ºC of temperature differences during the majority of night time hours between the rooftop and the exterior temperature (Figure *7*) proves this potential energy benefits could be further explored in the future.

Conclusions

Buildings and greenhouses are two of the main energy consumers worldwide. This work illustrated a way to improve energy efficiencies of both systems by integrating greenhouses in building's unoccupied roofs. The ICTA building has been used as a demonstrator in which data from 4 years and a calibrated energy model were assessed to investigate three energy-related scenarios. Simulation results indicated that the iRTG passively recovered an equivalent annual heating energy of 98 kWh/m^2 from the building (especially during nighttime) if heated with the same HVAC system of the ICTA building. Simulation work also demonstrated that the iRTG has an added insulation value especially in winter, which results in an annual energy saving of 35 kWh/m^2, equivalent to approximately 4% of the annual energy needs of ICTA. When taking into account the additional energy required to operate the building climate system in an integrated way to enable thermal exchange between iRTG and the building, the annual net energy gains for the whole system are 128 kWh/m^2. This is equivalent to 45.6 kg CO_2 eq/m^2 of carbon savings when benchmarked using the Spanish energy mix. Thermal analysis showed the potential usage of greenhouses as a sink for low grade building waste heat via the integration of the building HVAC systems with the greenhouse. Office building spaces are on average 4.7ºC warmer (October-May) and 3.2ºC cooler (June-September) than the iRTG. This presents a major potential for buoyancy (or mechanically) driven airborne thermal energy transfers across full annual cycle with no or minimal fan duties. Additionally, the iRTG acted as a solar collector and had daytime temperatures that were on average 5.1ºC warmer in winter when compared with other unheated building spaces. This excess solar energy can aid to heat the host building zones using an integrated HVAC system. The integration of rooftop greenhouses into unused spaces of urban fabric can aid to decarbonize both buildings and urban agriculture and improve the energy performance of the combined systems.

Acknowledgement

The authors are grateful to the Secretaria d'Universitats i Recerca del Departament d'Economia i Coneixement de la Generalitat de Catalunya for the award of a research scholarship (FI-DGR 2018) to Joan Muñoz-Liesa; to the Universitat Autònoma de Barcelona for the award of a research scholarship (PIF-2017) to Martí Rufí-Salís; to the Spanish Ministry of Economy and Competitiveness (MINECO) for the financial support to the research project Fertilectiy II "Integrated rooftop greenhouses: energy, waste and CO_2 symbiosis with the building. Towards foods security in a circular economy" (CTM2016-75772-C3-1-R; CTM2016-75772-C3-2-R). Authors also acknowledge financial support from the Spanish Ministry of Science, Innovation and Universities, through the "María de Maeztu" program for Units of Excellence (MDM-2015-0552). This work was additionally enabled by the Càtedra JG Ingenieros – Universitat Politècnica de Catalunya and the UK Engineering and Physical Sciences Research Council grand EP/P001173/1. Authors also thank Oriol Baeza, Prof. Xavier Gabarrell, Prof. Joan Rieradevall and the ICTA-UAB staff for their very valuable supporting advise and help.

743 ## Appendix

Parameter	Description
Heating	Ground source heat pumps
Heating setpoint (setback)	Seasonally adjusted (see section 2.2)
GSHP CoP [a]	3.5 (heating) – 2.5 (cooling)
Ventilation	Displacement natural ventilation (atrium and double skin facade) – mechanical ventilation in occupied zones.
Ventilation rate	12 litre/second/person as well as natural ventilation via openable windows
DHW consumption	1.2 litre/m^2/day
Cooling setpoint (setback)	Seasonally adjusted (see section 2.2)
Nominal lighting power density	3 W/m^2 (manually controlled) to achieve 200 lux
Occupant density	0.028 (p/m^2)
Internal gains	2.5 W/m^2 (combined office equipment and catering)
Gross (conditioned) area	7200m^2 (5040 m^2)
Observed annual electricity consumption (2015)	845,518 kWh
Fabric properties:	
Glazing type	Clear Polycarbonate
Glazing U-Value [b] (W/m^2K)	5.7
External walls [c] (W/m^2K)	1.1
Roof (W/m^2K)	5.7
Floor [d] (W/m^2K)	0.382
Infiltration (ac/h)	2
Clear Polycarbonate material [b]	
Thickness (mm)	0.8
Conductivity (W/mK)	0.2
Solar transmittance	0.835
Visible light transmittance	0.883

Parameter	Description
Total Infrared transmittance	0.800
Thermal-shading curtains [e]	
Emissivity	0.69
Transmissivity	0.19
Reflectivity	0.12
Soil condition (scenario 1) [f]	
Active thickness (mm)	490
Conductivity (W/m.K)	1.28
Specific heat (J/Kg.K)	880
Density (Kg/m^2)	1460
Thermal absorbance	0.9
Solar absorbance	0.7

Table A.1 Parameter inputs for energy model development of the case-study building

System	Item	Number of motors [g]	Power cons. (kW) [h]	Operations / day (avg) [i]	kWh / annually
Building 4th floor windows (inc 4 x iRTGs)	Façade lateral windows	16	0.11	2	24.98
	Roof windows	32	0.11	5	124.91
iRTGs thermal-shading curtains	Façades	8	0.09	2	26.28
	Atrium	4	0.09	2	13.14
	Roof	4	0.09	2	21.90
Siemens automation devices	Programmable logic controllers, inc. peripherical devices	4	0.005	24h	175.20
	Desigo Insight Server	1	0.264	24h	2312.64

System	Item	Number of motors [g]	Power cons. (kW) [h]	Operations / day (avg) [i]	kWh / annually
Air Handling Units (AHU) from 3rd floor laboratories	Input airflow from iRTG	4	1.1	24h / 11,000 m^3/h	30747.60
	Output airflow from laboratories	4	3.51	24h / 8,000 m^3/h	9636.00
TOTAL annual energy					3100
TOTAL annual energy / m^2 greenhouse					5.27

Table A.2 Energy inputs to operate passive and active (forced ventilation) building strategies.

Notes:

[a] From actual field measurements of GSHP as outlined in table 3 of [63].

[b] According to the material manufacture [83].

[c] Double skin façade made of similar material to glazing, with 900mm air cavity separating the skins modeled with 5% aluminum bridging.

[d] 75mm finished steel-reinforced concrete layer, 25mm expanded polystyrene, 380mm structural concrete incorporating 20mm air tubes.

[e] Manufacturers product technical literature as [12]

[f] ASHRAE Handbook -- Fundamentals - Physical Properties of Materials

[g] Accounted for all 4th floor, including the 4 iRTGs and the inner common space in between.

[h] According to building manufacturers product technical literature.

[i] According to building SQL historical data from 2015 to 2018 (assumed to be valid for 2015 only). Average roundup values for all same type of motors has been considered for the worst case (i.e., for the highest recorded value of all registered windows/curtains from the same type).

References

[1] European Commission, Energy Roadmap 2050. Impact assessment and scenario analysis (Commission staff working paper), Office for Official Publications of the European Communities, 2012.

[2] D. Connolly, B.V. Mathiesen, P.A. Østergaard, B. Möller, Heat Roadmap Europe 2050: Second pre-study for the EU27, Department of Development and Planning, Aalborg University, Denmark, 2013.

[3] U.N. Environment Programme, Buildings and Climate Change, UNEP/Earthprint, 2007.

[4] European Commission, EU Energy Commission Department, EU Buildings Database - Energy European Commission, Ec.Europa.Eu. (2016). https://ec.europa.eu/energy/en/eu-buildings-database (accessed October 5, 2019).

[5] European Commission, EU Energy Commission Department, New rules for greener and smarter buildings will increase quality of life for all Europeans, Ec.Europa.Eu. (2013) 1–8. https://ec.europa.eu/info/news/new-rules-greener-and-smarter-buildings-will-increase-quality-life-all-europeans-2019-apr-15_en (accessed December 25, 2019).

[6] European Union, Directive (EU) 2018/844 of the European Parliament and of the Council of 30 May 2018 amending Directive 2010/31/EU on the energy performance of buildings and Directive 2012/27/EU on energy efficiency, 2018.

[7] European Union, Directive 2012/27/EU of the European Parliament and of the Council of 25 October 2012 on energy efficiency, amending Directives 2009/125/EC and 2010/30/EU and repealing Directives 2004/8/EC and 2006/32/EC (Text with EEA relevance), Official Journal of the European Union. (2012) 1–56.

[8] European Union, Directive 2010/31/EU of the European Parliament and of the Council of 19 May 2010 on the energy performance of buildings, (2010) 1–23.

[9] IPCC, *Climate Change 2014: Synthesis Report. Contribution of Working Groups I, II and III to the Fifth Assessment Report of the*

Intergovernmental Panel on Climate Change, Intergovernmental Panel on Climate Change, Geneva, Switzerland, 2014.

[10] U.N.D.O.E.A.S.A. Population Division, World Urbanization Prospects: The 2018 Press Release, United Nations Publications, 2018.

[11] H. Girardet, Regenerative cities written for the world council and Hafen city University Hamburg (HCO) Commission on Cities and Climate Change. Ham-burg: Hafen ..., 2010. doi:10.1007/978-3-319-38919-6_9.

[12] A. Nadal, P. Llorach-Massana, E. Cuerva, E. López-Capel, J.I. Montero, A. Josa, et al., Building-integrated rooftop greenhouses: An energy and environmental assessment in the mediterranean context, Applied Energy. 187 (2017) 338–351. doi:10.1016/j.apenergy.2016.11.051.

[13] D. Gould, T. Caplow, Building-integrated agriculture: a new approach to food production, Woodhead Publishing Limited, 2012. doi:10.1533/9780857096463.2.147.

[14] F.J. Baptista, B.J. Bailey, J.F. Meneses, Effect of nocturnal ventilation on the occurrence of Botrytis cinerea in Mediterranean unheated tomato greenhouses, Crop Protection. 32 (2012) 144–149.

[15] B. Goldstein, M. Hauschild, J. Fernández, M. Birkved, Urban versus conventional agriculture, taxonomy of resource profiles: a review, Agron. Sustain. Dev. 36 (2016) 1–19. doi:10.1007/s13593-015-0348-4.

[16] B.J.P. Grard, C. Chenu, N. Manouchehri, S. Houot, N. Frascaria-Lacoste, C. Aubry, Rooftop farming on urban waste provides many ecosystem services, Agron. Sustain. Dev. 38 (2018) 898. doi:10.1007/s13593-017-0474-2.

[17] M. Rufí-Salís, A. Petit-Boix, G. Villalba, M. Ercilla-Montserrat, D. Sanjuan-Delmás, F. Parada, et al., Identifying eco-efficient year-round crop combinations for rooftop greenhouse agriculture, Int J Life Cycle Assess. 41 (2020) 89–576. doi:10.1007/s11367-019-01724-5.

[18] A. Piorr, I. Zasada, A. Doernberg, F. Zoll, W. Ramme, Research for AGRI Committee - Urban and peri-urban agriculture in the EU, Policy Department for Structural and Cohesion Policies; European Union. (2018) 1–89.

[19] A. Vadiee, V. Martin, Thermal energy storage strategies for effective closed greenhouse design, Applied Energy. 109 (2013) 337–343. doi:10.1016/j.apenergy.2012.12.065.

[20] P.J.M. van Beveren, J. Bontsema, G. van Straten, E.J. Van Henten, Optimal control of greenhouse climate using minimal energy and grower defined bounds, Applied Energy. 159 (2015) 509–519. doi:10.1016/j.apenergy.2015.09.012.

[21] European Environment Agency (EEA), Climate change adaptation in the agriculture sector in Europe, EEA Report. (2019) 1–112.

[22] C. Wallgren, M. Höjer, Eating energy—Identifying possibilities for reduced energy use in the future food supply system, Energy Policy. 37 (2009) 5803–5813. doi:10.1016/j.enpol.2009.08.046.

[23] L.F. Cabeza, L. Rincón, V. Vilariño, G. Pérez, A. Castell, Life cycle assessment (LCA) and life cycle energy analysis (LCEA) of buildings and the building sector: A review, Renewable and Sustainable Energy Reviews. 29 (2014) 394–416. doi:10.1016/j.rser.2013.08.037.

[24] E. Sanyé-Mengual, J. Oliver-Solà, J.I. Montero, J. Rieradevall, An environmental and economic life cycle assessment of rooftop greenhouse (RTG) implementation in Barcelona, Spain. Assessing new forms of urban agriculture from the greenhouse structure to the final product level, Int J Life Cycle Assess. 20 (2015) 350–366. doi:10.1007/s11367-014-0836-9.

[25] E. Sanyé-Mengual, P. Llorach-Masana, D. Sanjuan-Delmás, J. Oliver-Solà, A. Josa, J.I. Montero, et al., The ICTA-ICP Rooftop Greenhouse Lab (RTG-Lab): closing metabolic flows (energy, water, CO_2) through integrated Rooftop Greenhouses, in: Finding Spaces for Productive Cities. Proceedings of the 6th AESOP Sustainable Food Planning Conference, 2014: pp. 693–701. doi:10.13140/RG.2.1.5016.7206.

[26] J. Fiksel, Sustainability and resilience: toward a systems approach, Sustainability: Science, Practice and Policy. 2 (2017) 14–21. doi:10.1080/15487733.2006.11907980.

[27] T. Ramesh, R. Prakash, K.K. Shukla, Life cycle energy analysis of buildings: An overview, Energy & Buildings. 42 (2010) 1592–1600. doi:10.1016/j.enbuild.2010.05.007.

[28] C.K. Chau, T.M. Leung, W.Y. Ng, A review on life cycle assessment, life cycle energy assessment and life cycle carbon emissions assessment on buildings, Applied Energy. 143 (2015) 395–413. doi:10.1016/j.apenergy.2015.01.023.

[29] J.M. Choi, Y.-J. Park, S.-H. Kang, Temperature distribution and performance of ground-coupled multi-heat pump systems for a greenhouse, Renewable Energy. 65 (2014) 49–55. doi:10.1016/j.renene.2013.07.010.

[30] K.A. Joudi, A.A. Farhan, Greenhouse heating by solar air heaters on the roof, Renewable Energy. 72 (2014) 406–414. doi:10.1016/j.renene.2014.07.025.

[31] A. ELkhadraoui, S. Kooli, I. Hamdi, A. Farhat, Experimental investigation and economic evaluation of a new mixed-mode solar greenhouse dryer for drying of red pepper and grape, Renewable Energy. 77 (2015) 1–8. doi:10.1016/j.renene.2014.11.090.

[32] H.G. Mobtaker, Y. Ajabshirchi, S.F. Ranjbar, M. Matloobi, Solar energy conservation in greenhouse: Thermal analysis and experimental validation, Renewable Energy. 96 (2016) 509–519. doi:10.1016/j.renene.2016.04.079.

[33] M.J. Gupta, P.C. Energy, Effect of greenhouse design parameters on conservation of energy for greenhouse environmental control, Energy. 27 (2002) 777–794. doi:10.1016/S0360-5442(02)00030-0.

[34] J. Wang, S. Li, S. Guo, C. Ma, J. Wang, S. Jin, Simulation and optimization of solar greenhouses in Northern Jiangsu Province of China, Energy & Buildings. 78 (2014) 143–152. doi:10.1016/j.enbuild.2014.04.006.

[35] V.P. Sethi, S.K. Sharma, Survey and evaluation of heating technologies for worldwide agricultural greenhouse applications, Solar Energy. 82 (2008) 832–859. doi:10.1016/j.solener.2008.02.010.

[36] T. Mattila, S. Lehtoranta, L. Sokka, M. Melanen, A. Nissinen, Methodological Aspects of Applying Life Cycle Assessment to Industrial Symbioses, Journal of Industrial Ecology. 16 (2012) 51–60. doi:10.1111/j.1530-9290.2011.00443.x.

[37] M. Rufí-Salís, A. Petit-Boix, G. Villalba, D. Sanjuan-Delmás, F. Parada, M. Ercilla-Montserrat, et al., Recirculating water and nutrients in urban agriculture: An opportunity towards environmental sustainability and water use efficiency? Journal of Cleaner Production. (2020) 121213.

[38] K. Ackerman, R. Plunz, M. Conard, R. Katz, E. Dahlgren, P. Culligan, The Potential for Urban Agriculture in New York City, 2011.

[39] K. Specht, R. Siebert, I. Hartmann, U.B. Freisinger, M. Sawicka, A. Werner, et al., Urban agriculture of the future: an overview of sustainability aspects of food production in and on buildings, Agric Hum Values. 31 (2013) 33–51. doi:10.1007/s10460-013-9448-4.

[40] B. Goldstein, M. Hauschild, J. Fernández, M. Birkved, Testing the environmental performance of urban agriculture as a food supply in northern climates, Journal of Cleaner Production. 135 (2016) 984–994. doi:10.1016/j.jclepro.2016.07.004.

[41] K. Benis, I. Turan, C. Reinhart, P. Ferrão, Putting rooftops to use – A Cost-Benefit Analysis of food production vs. energy generation under Mediterranean climates, Cities. 78 (2018) 166–179. doi:10.1016/j.cities.2018.02.011.

[42] T. Weidner, A. Yang, M.W. Hamm, Consolidating the current knowledge on urban agriculture in productive urban food systems: Learnings, gaps and outlook, Journal of Cleaner Production. 209 (2019) 1637–1655. doi:10.1016/j.jclepro.2018.11.004.

[43] B. Sturm, M. Maier, M. Royapoor, S. Joyce, Dependency of production planning on availability of thermal energy in commercial greenhouses - A case study in Germany, Applied Thermal Engineering. 71 (2014) 239–247. doi:10.1016/j.applthermaleng.2014.05.095.

[44] Y. Thomas, L. Wang, A. Denzer, Energy Savings Analysis of a Greenhouse Heated by Waste Heat, Building Simulation. (2017). doi:10.26868/25222708.2017.713.

[45] SUEZ, The Decoset Syndicate and SUEZ Inaugurate the Heating Network in the Econotre Eco-pole: the First Tomato Greenhouses Heated by Energy Recovered from Household Waste [Press release], Httpswww.Suez.comen NewsPress-ReleasesEconotre. (2017) 1–2. https://www.suez.com/en/News/Press-Releases/Econotre (accessed January 20, 2020).

[46] J.I. Montero, E. Baeza, P. Muñoz, E. Sanyé-Mengual, C. Stanghellini, Technology for Rooftop Greenhouses, (2017) 83–101.

[47] N. Bibi-Triki, S. Bendimerad, A. Chermiti, T. Mahdjoub, B. Draoui, A. Abène, Modeling, characterization and analysis of the dynamic behavior of heat transfers through polyethylene and glass walls of greenhouses, Physics Procedia. 21 (2011) 67–74.

[48] M. Delor, Current state of building-integrated agriculture, its energy benefits and comparison with green roofs—summary, 2011.

[49] R. Ward, M. Jans-Singh, R. Choudhary, Quantifying the Environmental and Energy Benefits of Food Growth in the Urban Environment, in: T. Kozai (Ed.), Smart Plant Factory, 1st ed., Springer Singapore, Singapore, 2018: pp. 245–287. doi:10.1007/978-981-13-1065-2_17.

[50] T. Ten Doeschate, The potentials of a rooftop greenhouse for an existing mixed-use building towards energy neutrality, (2015).

[51] I. Cerón-Palma, Strategies for sustainable urban systems introducing eco-innovation in buildings in Mexico and Spain, Universitat Autònoma de Barcelona,, 2012.

[52] B. Bass, B. Baskaran, Evaluating Rooftop And Vertical Gardens as an Adaptation Strategy for Urban Areas, CCAF Impacts and Adaptatıon Progress Report, Institute for Research in Construction, Canada, n.d.

[53] N.H. Wong, A.Y.K. Tan, P.Y. Tan, N.C. Wong, Energy simulation of vertical greenery systems, Energy & Buildings. 41 (2009) 1401–1408. doi:10.1016/j.enbuild.2009.08.010.

[54] I. Jaffal, S.-E. Ouldboukhitine, R. Belarbi, A comprehensive study of the impact of green roofs on building energy performance, Renewable Energy. 43 (2012) 157–164. doi:10.1016/j.renene.2011.12.004.

[55] T. Caplow, J. Nelkin, Building-integrated greenhouse systems for low energy cooling, New York Sun Works. (2007).

[56] J. Muñoz-Liesa, M. Royapoor, E. López-Capel, E. Cuerva, S. Gassó-Domingo, A. Josa, Improving urban metabolism: Bi-directional energy and environmental benefits of rooftop greenhouse and building integration [In Press], 2019.

[57] M. Royapoor, A. Antony, T. Roskilly, A review of building climate and plant controls, and a survey of industry perspectives, Energy & Buildings. 158 (2018) 453–465. doi:10.1016/j.enbuild.2017.10.022.

[58] A. Prada, A. Gasparella, P. Baggio, On the performance of meta-models in building design optimization, Applied Energy. 225 (2018) 814–826. doi:10.1016/j.apenergy.2018.04.129.

[59] ASHRAE Guideline, Guideline 14-2014--Measurement of Energy, Demand, and Water Savings, American Society of Heating, Refrigerating, and Air Conditioning Engineers. (2014).

[60] M. Royapoor, T. Roskilly, Building model calibration using energy and environmental data, Energy & Buildings. 94 (2015) 109–120. doi:10.1016/j.enbuild.2015.02.050.

[61] S. Bonachela, A.M. González, M.D. Fernández, Irrigation scheduling of plastic greenhouse vegetable crops based on historical weather data, Irrig Sci. 25 (2006) 53–62. doi:10.1007/s00271-006-0034-z.

[62] S. Standard, Código Técnico de la Edificación. Documento Básico. Ahorro de Energía, CTE-DB-HE, 2006.

[63] M. Royapoor, H. Du, N. Wade, M. Goldstein, T. Roskilly, P. Taylor, et al., Carbon mitigation unit costs of building retrofits and the scope for carbon tax, a case study, Energy & Buildings. 203 (2019) 109415. doi:10.1016/j.enbuild.2019.109415.

[64] International Organization for Standardization, ISO 7730 2005-11-15 Ergonomics of the Thermal Environment, 2005.

[65] R. Tesi, Mezzi di protezione per l'ortoflorofrutticoltura ed il vivaismo, (1992).

[66] M. Ercilla-Montserrat, R. Izquierdo, J. Belmonte, J.I. Montero, P. Muñoz, C. De Linares, et al., Building-integrated agriculture: A first assessment of aerobiological air quality in rooftop greenhouses (i-RTGs), Science of the Total Environment. 598 (2017) 109–120. doi:10.1016/j.scitotenv.2017.04.099.

[67] J.J.G. Opdam, G.G. Schoonderbeek, E.M.B. Heller, A. de Gelder, Closed Greenhouse: a Starting Point for Sustainable Entrepreneurship in Horticulture, in: ActaHortic, International Society for Horticultural Science (ISHS), Leuven, Belgium, 2005: pp. 517–524.

[68] G. Proksch, Creating Urban Agricultural Systems, Routledge, 2017.

[69] J.C. Bakker, H.F. De Zwart, J.B. Campen, Greenhouse cooling and heat recovery using fine wire heat exchangers in a closed pot plant greenhouse: Design of an energy producing greenhouse, in: 2006: pp. 263–270. doi:10.17660/ActaHortic.2006.719.29.

[70] E. Terini, A. Dimitris, The contribution of a planted roof to thermal protection of building in Greece, Energy & Buildings. 27 (1998) 29–36.

[71] N.H. Wong, S.F. Tay, R. Wong, C.L. Ong, A. Sia, Life cycle cost analysis of rooftop gardens in Singapore, Building and Environment. 38 (2003) 499–509. doi:10.1016/S0360-1323(02)00131-2.

[72] S. Saiz, C. Kennedy, B. Bass, K. Pressnail, Comparative life cycle assessment of standard and green roofs, Environ. Sci. Technol. 40 (2006) 4312–4316. doi:10.1021/es0517522.

[73] N.H. Wong, S. Kardinal Jusuf, A. Aung La Win, H. Kyaw Thu, T. Syatia Negara, W. Xuchao, Environmental study of the impact of greenery in an institutional campus in the tropics, Building and Environment. 42 (2007) 2949–2970. doi:10.1016/j.buildenv.2006.06.004.

[74] M. Ottelé, K. Perini, A.L.A. Fraaij, E.M. Haas, R. Raiteri, Comparative life cycle analysis for green faÃ§ades and living wall systems, Energy & Buildings. 43 (2011) 3419–3429. doi:10.1016/j.enbuild.2011.09.010.

[75] K. Benis, C. Reinhart, P. Ferrão, Building-integrated agriculture (BIA) in urban contexts: testing A simulation-based decision support workflow, Conference Proceedings Ibpsa.org.

[76] A.N. Baytorun, Z. Zaimoglu, Climate Control in Mediterranean Greenhouses, in: Climate Resilient Agriculture - Strategies and Perspectives, InTech, 2018: pp. 1–17. doi:10.5772/intechopen.72367.

[77] D. Piscia, J.I. Montero, E. Baeza, B.J. Bailey, A CFD greenhouse night-time condensation model, 111 (2012) 141–154. doi:10.1016/j.biosystemseng.2011.11.006.

[78] Swiss Center for Life Cycle Inventories, Ecoinvent version 3.5 Life Cycle Inventory Database, (2018).

[79] G. Proksch, Creating Urban Agricultural Systems: An Integrated Approach to Design, (2016).

[80] L. Rathmell, Lufa Farms: A Model of Responsible Urban Agriculture, Resource Magazine. 20 (2013) 22.

[81] F. Orsini, M. Dubbeling, H. de Zeeuw, G. Gianquinto, Rooftop Urban Agriculture, Springer, 2018.

[82] C. Kubota, Growth, Development, Transpiration and Translocation as Affected by Abiotic Environmental Factors, in: Plant Factory: an Indoor Vertical Farming System for Efficient Quality Food Production, Elsevier, 2015: pp. 151–164. doi:10.1016/B978-0-12-801775-3.00010-X.

[83] J.Y. Choi, W.J. Kim, Significant effects of adding trace amounts of Ti on the microstructure and corrosion properties of Mg–6Al–1Zn magnesium alloy, Journal of Alloys and Compounds. 614 (2014) 49–55. doi:10.1016/j.jallcom.2014.06.052.

Highlights

⇒ Integrated greenhouses are a bioclimatic strategy to improve urban metabolism.

⇒ EnergyPlus proves bidirectional energy benefits for buildings and greenhouses.

⇒ iRTG recycle notable amounts of low-grade waste heat from buildings.

⇒ iRTGs acts as a solar collector and insulation cavity to reduce building energy.

⇒ Greenhouses can be integrated into building HVAC for improved efficiencies.

Declaration of interests

☒ The authors declare that they have no known competing financial interests or personal relationships that could have appeared to influence the work reported in this paper.

☐The authors declare the following financial interests/personal relationships which may be considered as potential competing interests: